SUPPORTING INFORMATION

Self-assembled Gold Nanoparticles and Amphiphile Peptides: A Colorimetric Probe for Copper(II) Ion Detection

Juliane N. B. D. Pelin,[a,b] Charlotte J. C. Edwards-Gayle,[b] Herculano Martinho,[a] Bárbara B. Gerbelli,[a] Valeria Castelletto,[b] Ian W. Hamley,[b] Wendel A. Alves[a],*

[a] *Centro de Ciências Naturais e Humanas, Universidade Federal do ABC, 09210-580, Santo André, Brazil*

[b] *Department of Chemistry, University of Reading, Reading RG6 6AD, United Kingdom*

Corresponding Author

*E-mail: wendel.alves@ufabc.edu.br

Table S1. Zeta potential for the hybrids $HAuCl_4/[RF]_4$ and $HAuCl_4/P[RF]_4$ synthesized using $NaBH_4$.

$HAuCl_4/[RF]_4$	Zeta Potential (mV)	$HAuCl_4/P[RF]_4$	Zeta Potential (mV)
6.7	+24.1 ± 0.49	6.7	+18.3 ± 0.15
3.3	+18.7 ± 0.46	3.3	+24.3 ± 0.10
2.3	+22.2 ± 0.19	1.7	+24.3 ± 0.05

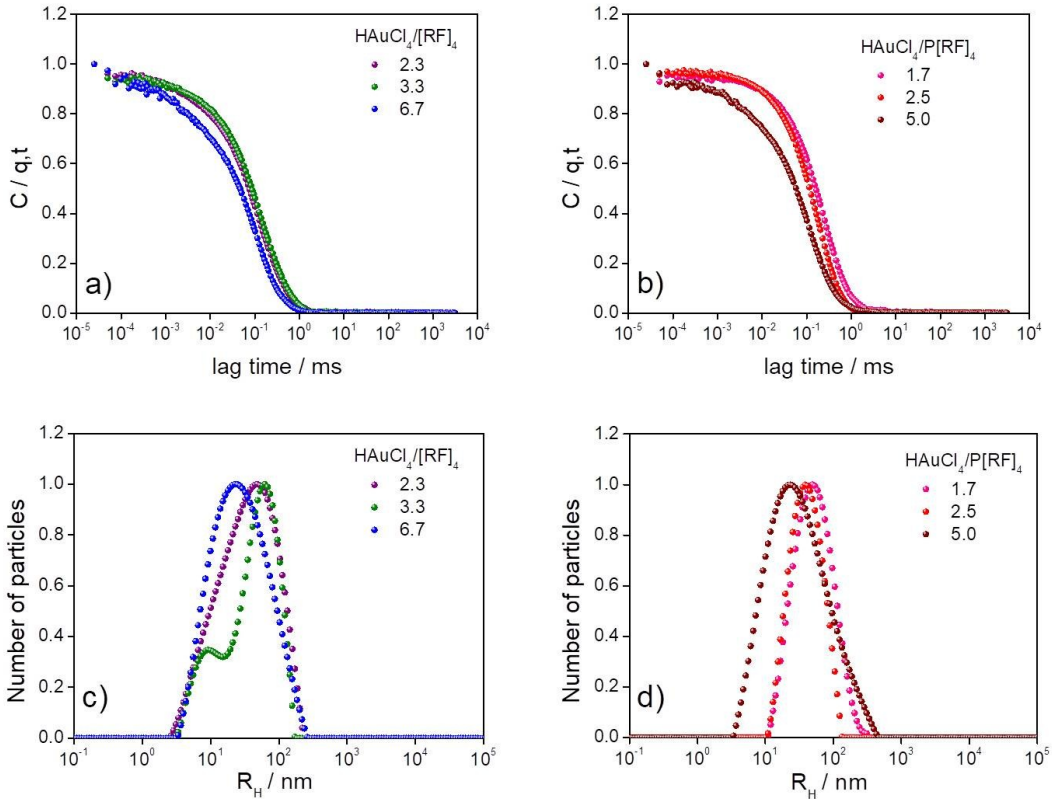

Figure S1. DLS correlation curves in the function of decay time for different proportion solutions of a) $HAuCl_4/[RF]_4$ and b) $HAuCl_4/P[RF]_4$, using $NaBH_4$. Curves of intensity distribution as a function of hydrodynamic radius for different proportion solutions of c) $HAuCl_4/[RF]_4$ and d) $HAuCl_4/P[RF]_4$, using $NaBH_4$.

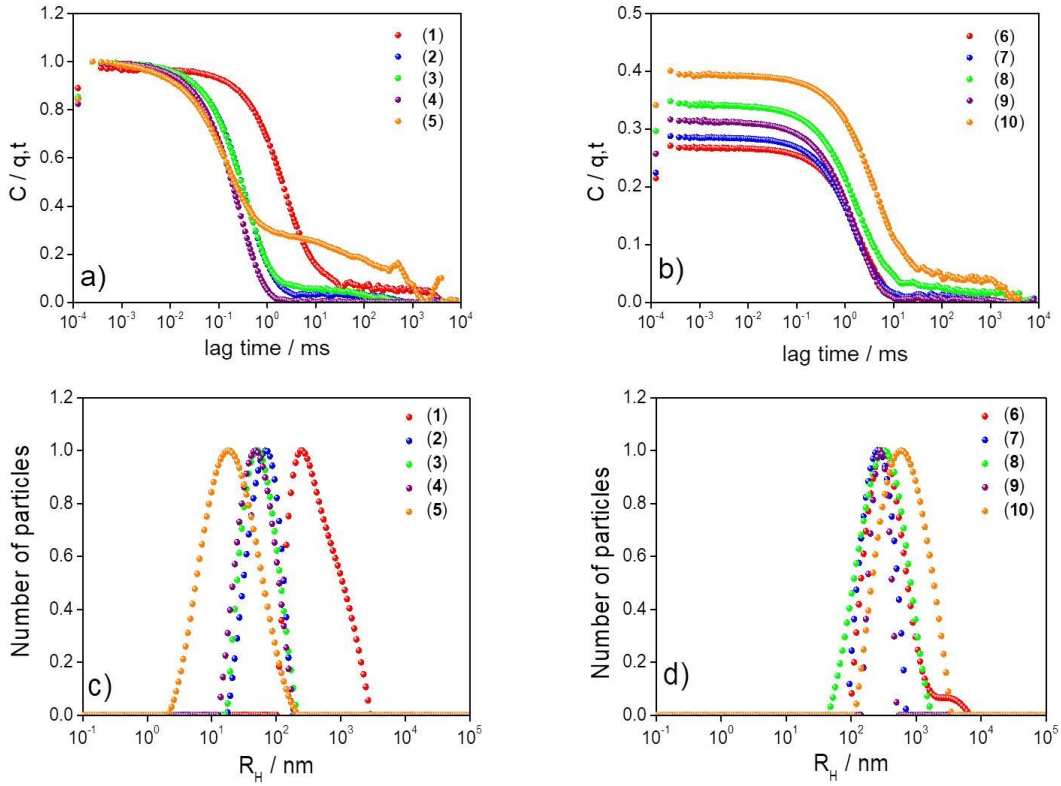

Figure S2. DLS correlation curves in the function of decay time for different $P[RF]_4/[RF]_4$ mixtures prepared with a) $HAuCl_4$-$NaBH_4$ and b) $HAuCl_4$-EGCG. Curves of intensity distribution as a function of hydrodynamic radius for different $P[RF]_4/[RF]_4$ mixtures prepared with c) $HAuCl_4$-$NaBH_4$ and d) $HAuCl_4$-EGCG.

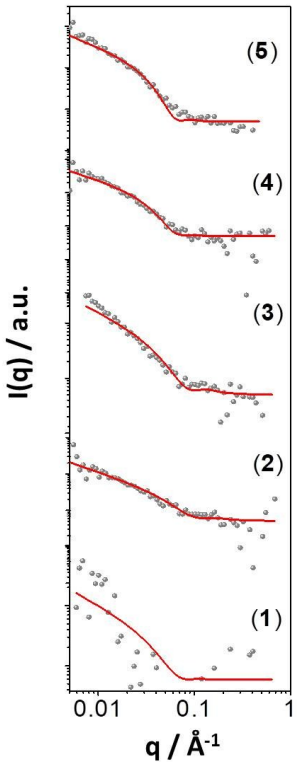

Sample	Long cylindrical shell				
	R (nm)	σ_R (nm)	ΔR (nm)	η_{core}	η_{shell}
(**1**)	3.7	0.3	0.6	2.9×10^{-8}	3.5×10^{-8}
(**2**)	1.7	0.5	0.5	5.0×10^{-8}	9.2×10^{-7}
(**3**)	2.0	0.6	0.6	1.4×10^{-9}	8.6×10^{-7}
(**4**)	4.1	0.7	0.7	9.2×10^{-8}	1.9×10^{-7}
(**5**)	5.0	0.5	0.6	1.1×10^{-7}	4.8×10^{-8}

Figure S3. SANS data (grey points) of $P[RF]_4/[RF]_4$ AuNP hybrids synthesized with $NaBH_4$ at pH 4. Model fits (red line) using the model described in the text. Table insert summarizes the fitting parameters obtained.

Figure S4. Lipopeptide blanks (left) and colour variations of the Cu^{2+} solutions (7.0, 15, 22, 30, 37, 45, 52, 60, 67, 75, 112, 150, and 223 µmol L^{-1}) and the systems (**1**), (**3**), (**5**), (**6**), (**8**), and (**10**) (right).

1

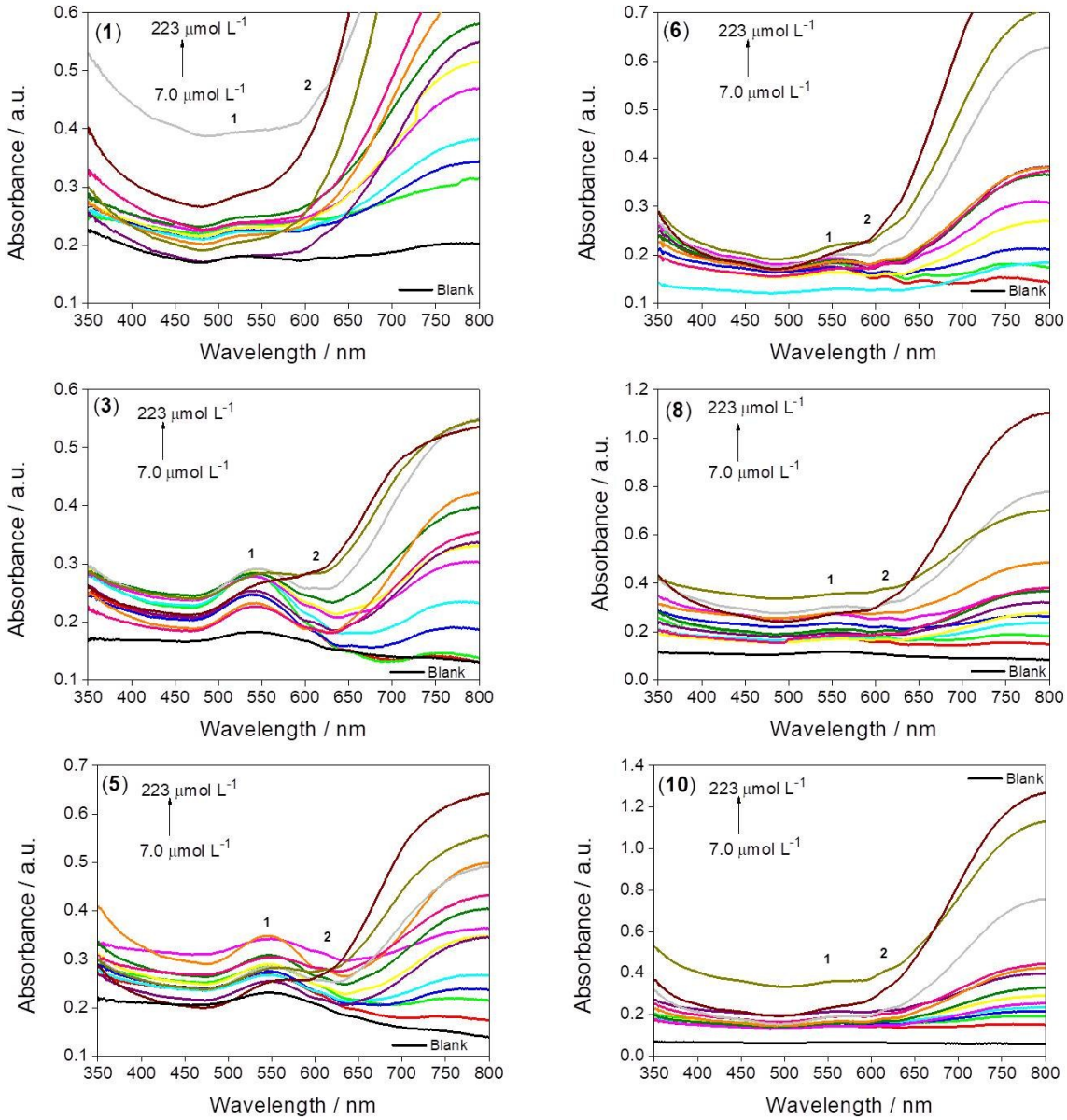

Figure S5. UV/Vis absorption spectra of the Cu^{2+} solutions (7.0, 15, 22, 30, 37, 45, 52, 60, 67, 75, 112, 150, and 223 μmol L^{-1}) in the systems (**1**), (**3**), (**5**), (**6**), (**8**), and (**10**).

Table S2. Raman bands assignment.

Vibrations (cm^{-1})	Assignments	References
107	Hydrogen-bond vibrations	[68]
170	N-Cu-N angle bend	[69]
214	Oriented crystal growth CuO	[70]
242	Cu-Cl bend	[69]
301	C-N vibrations	[60,61]
401	Cu-O stretch	[69]
434	Phenyl ring torsion	[62]
520	Silicon vibration	[66]
620	C-C twisting mode of the phenylalanine	[63]
831	C-H vibration	[64]
943	C-C vibration of the proline	[63]
985	Benzene ring breathing mode	[65]
1004	C-C vibration of the phenylalanine	[63]
1031	C-H vibration of the phenylalanine	[63]
1088	C-N vibrations of the proteins and aromatic C-C stretching	[63,66]
1158	N-H vibration of the arginine	[68]
1184	C-C stretching	[66]
1208	C-N stretching	[66]
1324	C-C stretching	[66]
1363	C-C stretching	[66]
1438	CH_2 deformation	[64]
1586	β-turn conformation	[64]
1607	β-turn conformation	[64]
1674	β-turn conformation	[64]
1698	β-turn conformation	[64]
1723	Ester carbonyl stretching	[67]

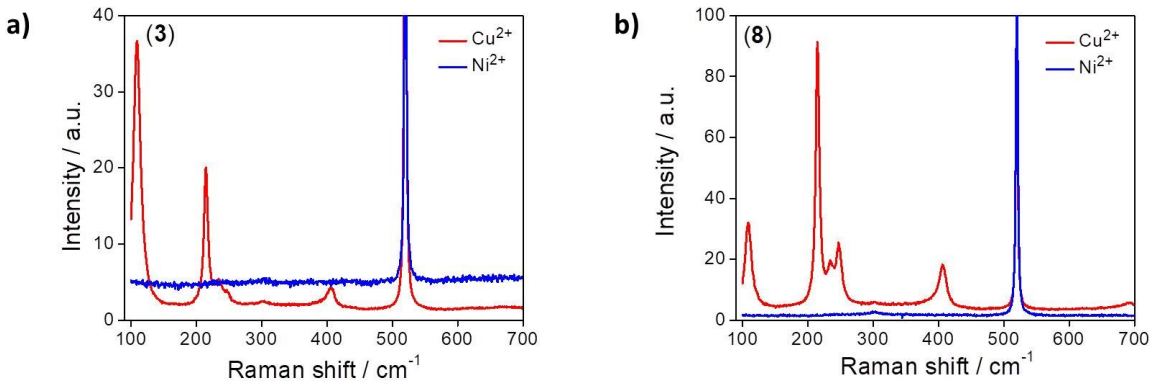

Figure S6. Comparison of the dispersive Raman spectra of 223 μmol L^{-1} solutions of Cu^{2+} and Ni^{2+}, for the systems (**3**), and (**8**).

Table S3. Estimate of Cu^{2+} concentration in water samples (rain and tap), using the (**1**), (**3**), (**5**), (**6**), (**8**), and (**10**) systems as metal ions probe.

Samples	**Rain**	**Tap**
	[Cu^{2+}] (µmol L^{-1})	**[Cu^{2+}] (µmol L^{-1})**
(**1**)	7.0 ± 0.07	7.0 ± 0.05
(**3**)	7.0 ± 0.03	7.0 ± 0.03
(**5**)	7.0 ± 0.02	15 ± 0.02
(**6**)	7.0 ± 0.05	7.0 ± 0.04
(**8**)	7.0 ± 0.02	15 ± 0.08
(**10**)	7.0 ± 0.07	15 ± 0.04